

0017-9310(94)00211-8

# A new way of obtaining heat and mass transfer at flat surfaces coated with swollen polymer by measuring recession with projected fringes

C. A. ROBERTS, J. R. LEECH† and N. S. GIRGIS

School of Engineering, Coventry University, Priory Street, Coventry CV1 5FB, U.K.

*(Received for publication in final form 29 July 1994)*

**Abstract**—The swollen polymer mass transfer technique has been applied with surface recession measurements being made by laser generated projected fringes, thus avoiding the need for holographic equipment. The technique proved to be successful for both plane and perforated surfaces. Results have been obtained for an air jet impinging on a flat plate and also for a model of the ligament plate which supports the tube mouths at the outlet of the flow reversal chamber in a shell boiler. When using a 2 mm polymer layer, surface recessions up to 40 microns are possible which can be measured to an accuracy of  $\pm 7$  microns. Contours of equal mass transfer are produced with this technique. The technique is useful for mass transfer coefficients up to  $0.01 \text{ m s}^{-1}$ . The results from both studies show agreement with those obtained by other methods.

## INTRODUCTION

The Chilton–Colburn analogy [1] can be used to convert measured mass transfer coefficients into heat transfer coefficients. For some years polymers swollen with organic liquids have been used as mass transfer surfaces [2–6] in experiments where it is the value of the heat transfer coefficient which is sought. These surfaces have the advantage over naphthalene that they can be reswollen for successive experiments. Also, surface recession during an experiment is much smaller than encountered with a subliming substance, perhaps as little as 10 microns [4], which will not disturb the flow. The theory of the swollen polymer method has been established by Macleod and his co-workers [7, 8] who have shown the significance of the constant rate period. During this period the pressure of the vapour above the surface of the swollen polymer remains effectively constant and equal to that above pure swelling agent; therefore the recession of the surface is directly proportional to the mass of swelling agent which is transferred.

In most previous studies the aim has been to use very thin layers of polymer and to permit minimal surface recession. Often holography has been used to measure the thickness, and hence the recession, of a transparent polymer. In some studies electronic speckle pattern interferometry has been used. The swollen polymer technique, unlike naphthalene sublimation, has been adopted and used by relatively few researchers, partly because of the demands of the optical systems which have been used. An attempt has been made in this work to extend the applicability of

the swollen polymer technique by combining it with an alternative optical measuring system. This has necessitated allowing larger recession to occur during an experiment, although not intentionally extending the experiment beyond the end of the constant rate period. The polymer and swelling agent combination used here permits a recession of up to 68 microns for a 2 mm polymer layer within the constant rate period for a very low flux rate of swelling agent from the surface. A recession of about 40 microns, as in the higher flux experiments reported here, is unlikely to alter the flow conditions significantly during an experiment, especially when the flow is unconfined. This recession, though small enough to cause insignificant disturbance to the flow, is large enough to enable use of a different optical measuring system. A 40 micron recession is greater than the recessions investigated and measured by researchers using holography but is still much less than those encountered when working with naphthalene.

With the alternative optical measuring system, projected fringes are observed on the surface of an opaque polymer. The projected fringes are generated by a robust optical system developed from work done on moiré fringes [9]. This is laboratory based but has the potential for portability.

As part of the development of the combined technique of mass transfer from swollen polymers measured by projected fringes, the mass transfer from a plane surface impinged by an air jet from a bell shaped nozzle has been investigated. Also studied has been the ligament plate in a model shell boiler. This plate featured an array of seven holes which were the mouths of the outlet tubes from the flow reversal chamber. Air flow from the chamber impinged nor-

† Author to whom correspondence should be addressed.

## NOMENCLATURE

$A$	surface area [m <sup>2</sup> ]	$R_o$	universal gas constant
$C_a$	concentration of swelling agent vapour in bulk air flow [kg m <sup>-3</sup> ]	$Re_D$	Reynolds number based on diameter
$C_s$	concentration of swelling agent vapour, which has partial pressure $p_s$ , in air–vapour mixture at polymer surface [kg m <sup>-3</sup> ]	$s$	fringe shift observed on viewed surface [microns]
$C(x, t)$	concentration of swelling agent in polymer at depth $(L - x)$ and time $t$ expressed as mass of swelling agent per unit volume of dry polymer and having the value $C_o$ at $x = L$ and $t = 0$	$t$	time [s]
$d$	projected fringe spacing [microns]	$T$	temperature [K]
$D$	viewed fringe spacing on polymer surface [microns]	$V_{py}, V_{sa}$	volume of polymer, swelling agent in swollen polymer [m <sup>3</sup> ]
$D$	diameter [m]	$\Delta z$	surface recession, i.e. change in swollen polymer thickness due to loss of swelling agent [microns]
$D, D_m$	diffusion coefficient, mass diffusivity [m <sup>2</sup> s <sup>-1</sup> ]	$z_1(x), z_2(x)$	functions describing initial, final surface profiles.
$F_s$	flux of swelling agent from swollen polymer surface [kg m <sup>-2</sup> s <sup>-1</sup> ]		
$h$	heat transfer coefficient [W m <sup>-2</sup> K <sup>-1</sup> ]		
$h_m$	mass transfer coefficient [m s <sup>-1</sup> ]		
$H$	distance of jet exit from surface upon which jet impinges [m]		
$I_1, I_2$	intensity observed for initial, final fringe patterns		
$L$	dry polymer thickness [m]		
$m$	mass [kg]		
$M_s$	molar mass of swelling agent vapour [kg]		
$p_s$	partial pressure of swelling agent vapour [Pa]		
$p_o$	partial pressure of swelling agent vapour in air–vapour mixture at surface of saturated swollen polymer (= partial pressure of vapour in air–vapour mixture above pure liquid swelling agent) [Pa]		
		<i>Greek symbols</i>	
		$\theta$	angle of projection of fringes measured relative to the normal to the surface on which the fringes are viewed [° or rad]
		$\rho_{sa}$	density of pure liquid swelling agent [kg m <sup>-3</sup> ]
		$\rho_{sp}$	density of swollen polymer [kg m <sup>-3</sup> ]
		$\phi_{sa}$	volume fraction of swelling agent in the swollen polymer, $V_{sa}/(V_{py} + V_{sa}) = 1 - \phi_{py}$
		$\phi_{sat}$	value of $\phi_{sa}$ for fully saturated swollen polymer
		$\phi_{1s}, \phi_{2s}$	surface values of $\phi_{sa}$ at start, end of experiment (vapour pressure 100% at start, 95% at end)
		$\chi$	Flory–Huggins parameter, characteristic of polymer–swelling agent combination
		$\omega$	phase describing the viewed fringe intensity, $(2\pi/D)(x + z(x) \tan \theta)$ [rad].

mally on the plate and an area around the central hole was studied. The aim of the work was to develop the combined measurement technique and to obtain data for the shell boiler configuration, for which there are few published data.

#### MASS TRANSFER FROM SWOLLEN POLYMERS

An opaque white silicone polymer (RTV 11 manufactured by GEC Silicones) was chosen as the mass transfer surface. This polymer adhered reliably to primed aluminium and could be cast by pouring it on to a test surface or injecting into a mould for curing. The swelling agent used was an ester, isobutyl benzoate. The volume fraction of swelling agent in the saturated swollen polymer at equilibrium was 0.2. The test samples investigated were 2 mm thick before swelling.

The swollen RTV 11 polymer provided a matt surface on which to view the distortion of the projected fringe patterns.

The equation for mass transfer rate may be written as follows:

$$\frac{dm}{dt} = h_m A (C_s - C_a) = \frac{\Delta z A}{t} \rho_{sa}$$

where  $C_a \approx 0$ . Here the density of pure swelling agent is used, assuming the swollen polymer conforms to the principle of additivity [10]. For very small  $\Delta z$ , there is some evidence that density  $\rho_{sp}$  should be used [4, 10].

The concentration of vapour with partial pressure  $p_s$  in a mixture of air and vapour at the swollen polymer surface [4] is  $C_s = (M_s p_s)/(R_o T)$ . Therefore

$$h_m = \frac{8.3T\Delta z \rho_{sa}}{M_s p_s t} \quad (1)$$

Thus  $h_m$  can be determined from the recession  $\Delta z$  which occurs during time  $t$  that the swollen polymer is exposed to the air flow. For most experiments in a cold flow model  $T$  is 293 K. For isobutyl benzoate  $M_s$  is 0.17823 kg,  $p_s$  is 4.61 N m<sup>-2</sup> [10] and  $\rho_{sa}$  is 1000 kg m<sup>-3</sup>. It follows that  $h_m = 2.96\Delta z/t$ .

Larger recessions ( $\Delta z > 50$  microns), though easier for the proposed optical system to measure, might be preferably studied by moiré methods. The latter would provide surface recession contours, and hence mass transfer coefficient contours, directly. Larger recessions, however, cause two particular problems. Greater permissible recession is achieved only at the expense of greater initial swelling which makes casting or moulding polymer on to complex surfaces difficult. This is because of the change which takes place to the geometry of the prepared model when the polymer swells. Also, the flow boundary conditions will be modified from the initial conditions by large recessions which take place during an experiment.

From the diffusion equation it is possible to deduce the maximum permissible recession for various flux rates of swelling agent leaving the swollen polymer surface. It is necessary to estimate the maximum permissible recession, and hence the duration of experiment for a particular flux rate for a particular thickness of polymer. This is to ensure that large recession experiments do not extend beyond the constant rate period for the polymer.

Calculations to find a predicted value for the maximum permissible recession can be performed as follows. The Flory-Huggins equation [11] strictly describes the behaviour of non-cross linked polymers. The equation can be expressed [7] in the form

$$\ln(p_s/p_o) = [\ln \phi_{sa} + (1 - \phi_{sa}) + \chi(1 - \phi_{sa})^2] \quad (2)$$

The validity of the use of this equation for cross-linked polymers has been previously discussed by others [7, 12, 13].

The constant  $\chi$  is a characteristic of a particular polymer-swelling agent combination. Except at the start of an experiment when the polymer is fully saturated, the surface value of  $\phi_{sa}$  will be less than  $\phi_{sat}$  and  $p_s$  will be less than  $p_o$ :

$$\ln 1 = \ln \phi_{1s} + (1 - \phi_{1s}) + \chi(1 - \phi_{1s})^2 \quad (3)$$

$$\ln 0.95 = \ln \phi_{2s} + (1 - \phi_{2s}) + \chi(1 - \phi_{2s})^2 \quad (4)$$

Rearranging equations (3) and (4) above [12] gives:

$$\chi = [\ln(1/\phi_{1s}) - 1 + \phi_{1s}]/(1 - \phi_{1s})^2 \quad (5)$$

$$\chi = [\ln(0.95/\phi_{2s}) - 1 + \phi_{2s}]/(1 - \phi_{2s})^2 \quad (6)$$

and similar equations for other  $p_s/p_o$  ratios. These relationships can be used to generate a family of curves with  $\chi$  plotted against  $\phi_{sa}$  for each  $p_s/p_o$  ratio. An inspection of these plots provides a value for the volume fraction of swelling agent at the surface after an experiment which ends when  $p_s$  has fallen from  $p_o$  by

a specified percentage, provided that the constant  $\chi$  is known for the polymer-swelling agent combination in use. This constant is found from an experimental value for  $\phi_{sat}$  and use of equation (2) with  $p_s/p_o$  equal to 1.

For RTV 11 and isobutyl benzoate, corresponding values are  $\phi_{sat} = 0.2$  and  $\chi = 1.26$ . Values for  $\phi_{sa}$  at the polymer surface are 0.1775 (for 95% vapour pressure), 0.160 (for 90%), 0.1425 (for 85%) and 0.128 (for 80%). A better swelling ratio would be  $\phi_{sat} = 0.3$  and  $\chi = 1.03$ , although a polymer with this property in addition to other requirements was not identified. For this higher degree of swelling, values for  $\phi_{sa}$  at the polymer surface would be 0.253 (for 95% vapour pressure), 0.220 (for 90%), 0.195 (for 85%) and 0.172 (for 80%).

Using a solution of the diffusion equation presented by Crank [14] it is possible to find the experiment duration and flux which together cause the prescribed fall in volume fraction of swelling agent at the surface. The diffusion coefficient for the swelling agent in the polymer must be known. This can be found from a simple swelling and weighing experiment following the method described by Kapur [12].

Equation (7) below was presented by Crank [14]:

$$C(L, t) = C_o - \frac{tF_s}{L} - \frac{LF_s}{3D} + \frac{2LF_s}{\pi^2 D} \sum_{n=1}^{n=\infty} \{fn\} \quad (7)$$

where

$$\{fn\} = \frac{(-1)^n}{n^2} \exp\left[\frac{-Dn^2\pi^2 t}{L^2}\right] \cos n\pi.$$

An expression of the form  $\phi_{sa}\rho_{sa}/(1 - \phi_{sa})$  is substituted for concentrations  $C(L, t)$  and  $C_o$ :

$$\frac{\phi_{sa}(L, t)}{1 - \phi_{sa}} = \frac{\phi_{sa}(L, 0)}{1 - \phi_{sa}} - \frac{F_s t}{L\rho_{sa}} - \frac{F_s L}{3D\rho_{sa}} + \frac{2F_s L}{\pi^2 D\rho_{sa}} \sum_{n=1}^{n=\infty} \{fn\} \quad (8)$$

From equation (8) it is possible, for a particular flux value  $F_s$ , to deduce at what time  $t$  the value of  $\phi_{sa}(L, t)$  falls, for example, to 0.1775 if  $\phi_{sa}(L, 0)$  is 0.2 or to 0.253 if  $\phi_{sa}$  is 0.3. The results of this calculation are plotted graphically in Fig. 1 for  $L$  values of 1 and 2 mm dry polymer thickness, using  $D = 6.4 \times 10^{-11}$  m<sup>2</sup> s<sup>-1</sup> and  $\rho_{sa} = 1000$  kg m<sup>-3</sup>. It can be seen that high maximum permissible recessions are attainable only for very low flux rates.

This calculation is necessary because swollen polymers have been used here differently from previous researchers. In past studies, the aim has been to use very thin layers of polymer, and users have measured very small recessions with very sensitive, usually optical, techniques. Here the objective has been to allow greater recession, using thicker layers of polymer to enable this, so that measurements can be made with a non-contact robust surface measuring system which can contour an opaque surface. This optical system is now described.

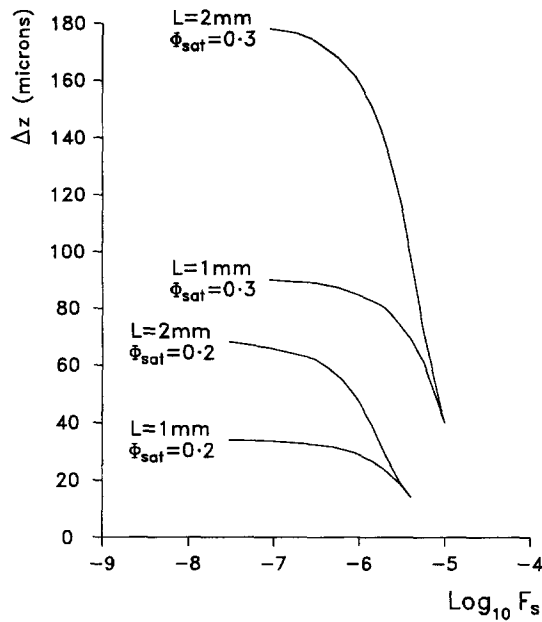


Fig. 1. Maximum permissible surface recessions as a function of  $\log_{10}$  flux for two different polymer thicknesses and initial degrees of saturation.

**OPTICAL MEASUREMENT TECHNIQUE**

A projected fringe system originally used for moiré interferometry has been developed for making surface topography measurements. When fringes of spacing  $d$  are projected obliquely at angle  $\theta$  on to a surface, then a fringe pattern of spacing  $D$  will be observed if the surface is viewed normally. From Fig. 2 it is apparent that  $d/D = \cos \theta$ . If the surface on which the fringe pattern is observed recesses by an amount  $z$ , then the observed pattern is shifted laterally by  $s$  where  $s/z = \tan \theta$ .

With large surface recessions, comparison of the patterns observed on the polymer surface before and after the application of an air flow would produce moiré fringes; the comparison could be performed by subtraction of intensities on a pixel by pixel basis. Moiré fringes would follow the contours of the recessed surface, but only for sufficiently large surface recessions. Smaller recessions of swollen polymer sur-

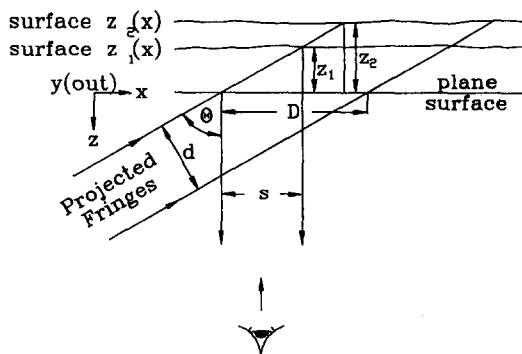


Fig. 2. The geometry of the optical measuring system.

faces can be measured by phase mapping [9, 15]. As the surface recesses it intersects the projected fringes at different points and the phase observed by normal viewing of each point changes as the surface recedes. These phase changes can be measured.

The phase mapping technique is implemented by using phase stepping. The observed fringe patterns on the polymer surface can be described by the following equations:

$$I_a = A + B \cos \omega \tag{9}$$

$$I_b = A + B \cos (\omega + 2\pi/3) \tag{10}$$

$$I_c = A + B \cos (\omega + 4\pi/3) \tag{11}$$

where phase  $\omega = (2\pi/D)(x + z \tan \theta)$ . Hence

$$\tan \omega = \sqrt{3(I_c - I_b)/(2I_a - I_b - I_c)}. \tag{12}$$

And thus  $z$  can be found as a function of  $x$ . It is necessary to measure the surface topography before and after an experiment in order to deduce surface recession  $\Delta z$ .

The fringe pattern observed on the initial surface is described by equation (9):

$$I_1 = A + B \cos \omega_1 = A + B \cos [(2\pi/D)(x + z_1(x) \tan \theta)].$$

When the surface recesses, it moves to a new position defined by

$$z_2(x) = z_1(x) + \Delta z$$

where  $\Delta z$  is negative for recession. The fringe pattern observed on the final surface is described by

$$I_2 = A + B \cos \omega_2 = A + B \cos [(2\pi/D)(x + z_2(x) \tan \theta)].$$

Therefore

$$\omega_2 - \omega_1 = (2\pi/D)(z_2(x) - z_1(x)) \tan \theta. \tag{13}$$

So surface recession

$$\begin{aligned} \Delta z &= \frac{\Delta \omega}{\frac{2\pi}{D} \tan \theta} \\ &= \frac{\Delta \omega}{\frac{2\pi \sqrt{(D^2 - d^2)}}{D d}} \end{aligned}$$

(from geometry, see Fig. 2)

$$\Delta z \approx \frac{\Delta \omega d}{2\pi} \quad (\text{if } d \ll D). \tag{14}$$

This approximation is correct for oblique fringe projection where  $\theta$  is greater than  $80^\circ$ . The value of  $\Delta z$  depends only on the measured phase difference and the projected fringe spacing  $d$ . The observed fringe spacing of  $D$  pixels on the monitor screen and the monitoring system sensitivity in microns/pixel are measured to find the angle of projection  $\theta$  and to verify that it is greater than  $80^\circ$ .

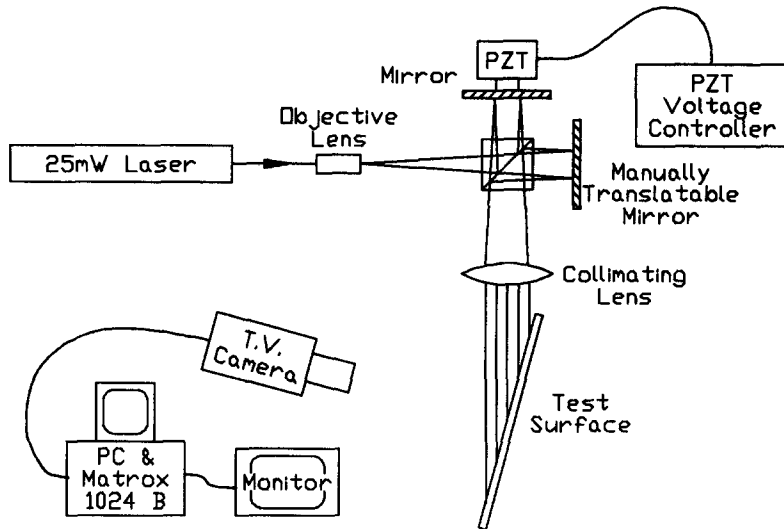


Fig. 3. Schematic diagram of the optical measuring system.

Consider a typical experiment where projected fringe spacing  $a$  is 254 microns. If the observed fringe spacing is 25 pixels and the monitoring system sensitivity is 200 microns/pixel, then  $D$  is 5000 microns. Thus  $\theta = \arccos(d/D) = 87.09^\circ$ . It is permissible therefore to use equation (14), which shows that for a surface recession  $\Delta z$  of 40 microns (near the maximum permissible) then  $\Delta\omega$  is approximately 1.0. Thus the phase shifts which the phase mapping technique must detect are less than 1/6 of a fringe. In the above example this is equivalent to a fringe lateral shift of four pixels. The most oblique fringe projection angle used in experiments is  $88^\circ$  as beyond that fringe intensity is low. In that case a 40 micron surface recession causes the image of the observed fringe pattern to shift laterally by about six pixels.

A schematic diagram of the optical measuring system is given in Fig. 3. The fringes are produced by a 25 mW He-Ne laser and a Michelson interferometer and are projected on to the polymer surface at an oblique angle. A 254 micron graticule is used to check the fringe spacing. Images of the fringes on the polymer surface are observed with a high resolution vidicon camera viewing the surface normally and are snatched by a Matrox PIP-1024B frame grabber. One of the interferometer mirrors is mounted on a piezoelectric translator (PZT) to enable phase stepping. Three frames (phase shifted by  $0, 2\pi/3$  and  $4\pi/3$ ) are snatched before the experiment to identify the features of the polymer surface. A further three frames are stored after the experiment. Computer analysis provides the change in the polymer surface topography.

#### EXPERIMENTAL MEASUREMENTS ON SWOLLEN POLYMER SURFACES

Encouraging results were obtained when flat polymer-coated surfaces were subjected to simple air jet

impingement [16]. The projected fringe method enabled the surface recession to be measured with an accuracy of about 7 microns. A moving average smoothing technique was added to the data processing to remove fluctuations with spatial frequency equal to half of the observed fringe spacing. These were attributable to inadvertent small errors in the setting of the PZT [17]. A batch of surface profiles was presented as contours of equal surface recession. The method was used to make further investigations of the normal impingement of an air jet from a bell shaped nozzle on a flat plate. Observations were made for air flow defined by the value of  $Re_D$  at the nozzle exit and for  $H/D$  defining the jet position relative to the plate.

In some additional studies, mass transfer in a model shell boiler was investigated. Heat transfer coefficients for the exit region of the combustion chamber, especially in the vicinity of the outlet tube mouths, were required. Measurements were made across an idealised ligament plate (Fig. 4) which supported the tubes at the exit from the combustion chamber but without protrusions corresponding to the welds which occur in a practical system. Mass transfer for  $Re_D$  range of 5000–15 500 in the outlet tubes was studied.

In all the tests the polymer coated surfaces were soaked for 24 hours in isobutyl benzoate. After careful drying the flat plate was mounted in a stand or the ligament plate was refitted in the model shell boiler. In the latter case, the fringe pattern projected on the surface was monitored throughout the timed passage of air in the experiment. An area up to  $10 \text{ cm} \times 1.3 \text{ cm}$  could be studied. In the model shell boiler, studies were on the area directly above, to the side and below the centre hole.

#### RESULTS OF TESTS ON PLANE FLAT PLATES

Surface recession contours obtained on flat plates are shown in Fig. 5(a)–(d). The form of the surface

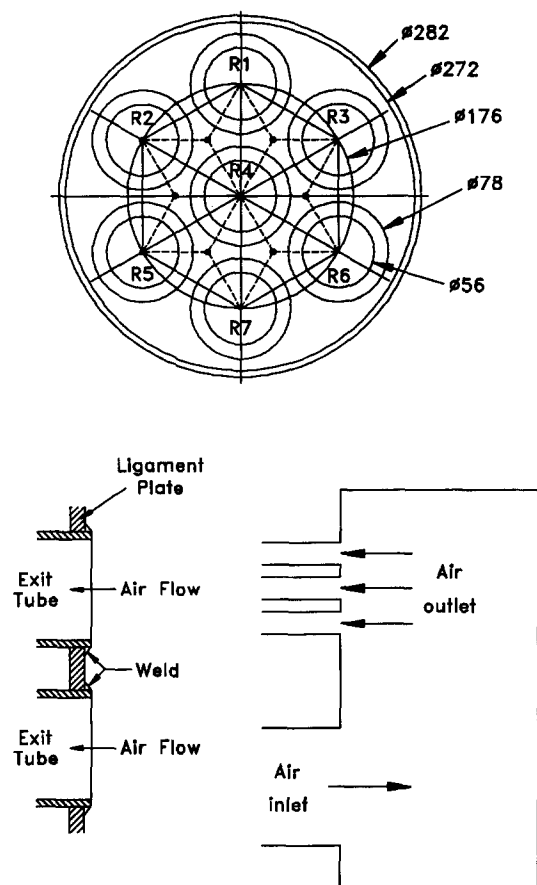


Fig. 4. Schematic diagram of model boiler and ligament plate geometry.

recession is discernible from the contours. The results are comparable with another study using a bell shaped nozzle by Popiel and Boguslawski [18].

In all these tests the velocity of air emerging from the 3.91 mm diameter bell shaped nozzle gave  $Re_D$  of 23 000 at exit. For Fig. 5(a) and (b) the  $H/D$  ratio was 1.3 and the air temperature 19.5°C. The contours in Fig. 5(a) are for a 20 min experiment; those in Fig. 5(b) are for a 10 min experiment. For Fig. 5(c) and (d) the  $H/D$  ratio was 7.0. The contours in Fig. 5(c) are for a 20 min experiment at 22°C and those in Fig. 5(d) for a 10 min experiment at 19.5°C.

The surface recession contours were at 7 micron intervals and were converted to mass transfer coefficients using equation (1). The dots along the side of the contour plots indicate 10 pixel intervals in the  $y$ -direction. The dark area to the right hand side of the contour maps (Fig. 5) has recessed by  $0 \pm 7$  microns. This was a reference area of masked, and hence unrecused, polymer.

In Fig. 5(a) and (b) the contours show a structure where mass transfer increases towards the centre of jet impingement, then decreases before increasing again at the centre. The contours indicate an annular area of higher mass transfer, then another annular area corresponding to lower mass transfer closer to

the centre, with high mass transfer at the centre. This feature of jet impingement is also clearly shown by the results of Popiel and Boguslawski [18]. In Fig. 5(a) the ring diameters were 20.62 and 15.64 mm, i.e. 5.3 and 4.0 jet diameters, respectively. In Fig. 5(b) the ring diameters were 17.96 and 12.93 mm, i.e. 4.6 and 3.3 jet diameters, respectively. From ref. [18] 4.9 and 3.7 jet diameters would have been the ring diameters for  $H/D$  1.2 and  $Re_D$  21 400. The rings observed here are in fair agreement with that, one result suggesting slightly larger diameters and the other slightly smaller.

The contours in Fig. 5(c) and (d) are for tests where  $H/D$  is equal to 7.0. No rings are observed. Surface recession takes the form of a simple depression which is in agreement with ref. [18].

In all cases the recessions observed were generally rather less than expected from a consideration of the work of Popiel and Boguslawski [18]. Their graph of Sherwood number versus jet diameter for  $H/D$  1.2 and  $Re_D$  21 400 had a maximum value near 100. Using  $5 \times 10^{-6}$  as a typical value for the mass diffusivity of swelling agent vapour in air, this Sherwood number corresponds to a maximum  $h_m$  of  $0.128 \text{ m s}^{-1}$  which should be compared with Fig. 5(a) and (b). Their graph of Sherwood number versus jet diameter for  $H/D$  7.0 and  $Re_D$  of 20 000 had a maximum value near 170. This corresponds to a maximum  $h_m$  of  $0.220 \text{ m s}^{-1}$  which should be compared with Fig. 5(c) and (d). The experiments had been allowed to continue for long enough to provide a measurable recession in order to test the optical measuring system. Because of this, these studies, which were high flux in nature, went beyond the end of the constant rate period, refer back to Fig. 1. It was judged that these experiments were successful in that the results offered fair qualitative agreement with previous data [18] and showed the existence of surface detail at low  $H/D$  value. It was anticipated that the mass transfer in the shell boiler model proposed for study was likely to be much lower than in the jet studies and that it would provide broad areas of differing degrees of mass transfer to be measured rather than fine surface detail.

#### RESULTS OF TESTS ON PLATES PERFORATED WITH HOLES IN MODEL BOILER

The holes in the flat ligament plate had diameter 56 mm and were arranged symmetrically with a pitch spacing of 88 mm. The relative location of the holes is given in Fig. 4. Typical contour maps are shown in Fig. 6(a–d), with their locations mapped in Fig. 7. A full set of results is presented elsewhere [19]. All the observations were made in the region of the central hole. Figure 6(a) is a study to the left side of R4 for  $Re_D$  of 5800 over 3 h at 20.25°C. Figure 6(b) is a study below R4 with  $Re_D$  of 10 600 for 2 h at 19.5°C. Figure 6(c) is also a study below R4 with  $Re_D$  of 15 250 for 2 h at 17.25°C. Figure 6(d) is a study above R4 with  $Re_D$  of 10 050 for 2 h at 20.0°C.

In Fig. 6(a) an unrecused (masked) area appears

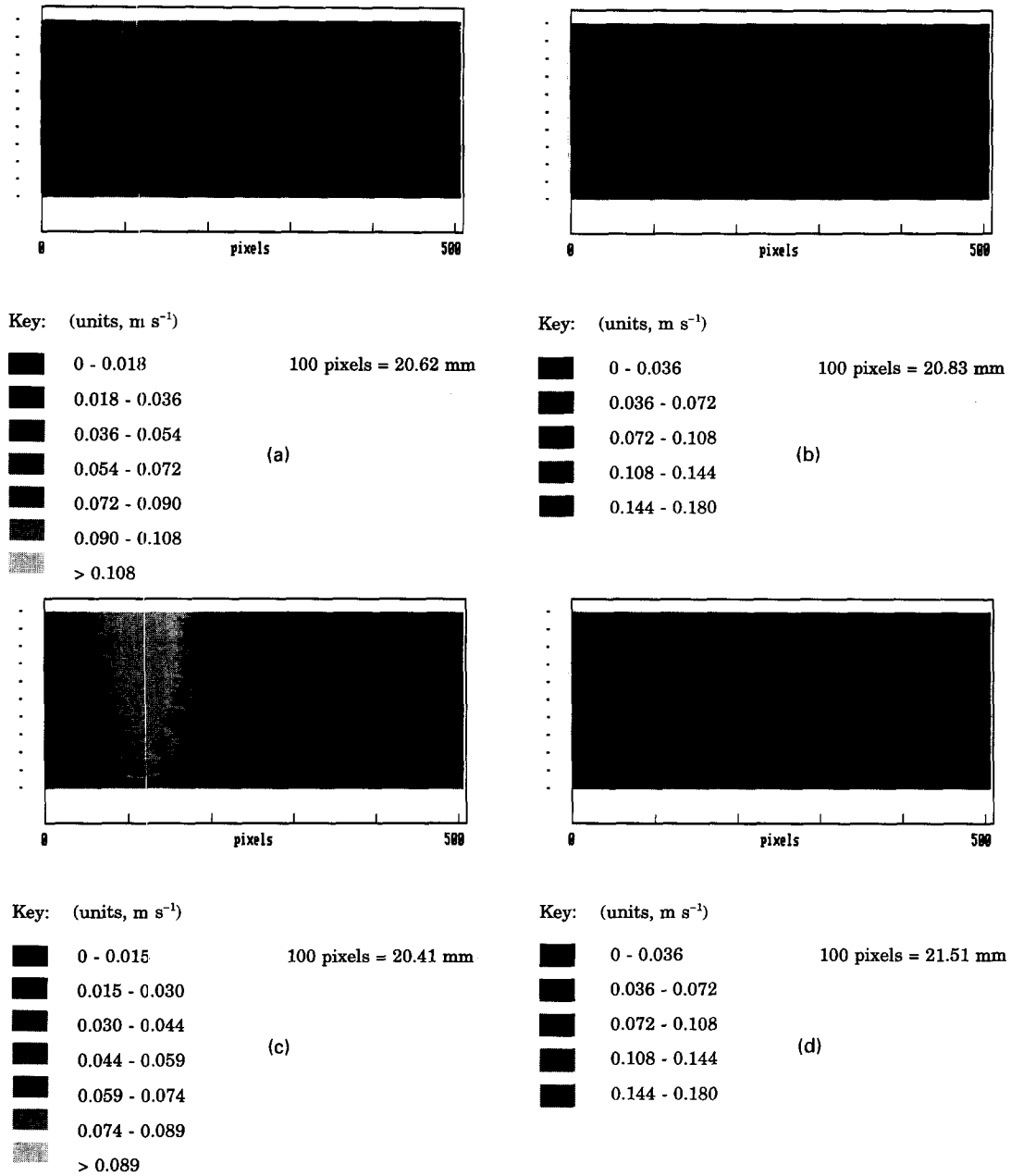


Fig. 5. Mass transfer contours obtained for air jet impingement (original in colour).

as a dark area on the left of the contour plot and the edge of hole R4 is on the right. The mask covered an area between hole R2 and the boiler wall on the left hand side. In Fig. 6(b) and (c) the bottom of hole R4 is studied. An area between holes R5 and R7 was masked. In these figures only the part of the contour adjacent to the lower part of hole R4 is shown. In Fig. 6(d) the top of hole R4 is studied. The mask covered an area between holes R1 and R2 but in this figure only the contours adjacent to the upper part of hole R4 are shown.

**DISCUSSION**

The results obtained for the model shell boiler surfaces can be compared with the very limited amount

of other data available, from work using naphthalene [20] and from more recent liquid crystal studies [21].

The earlier work [20] investigated a flat plate but pitch/diameter ratios were 2.0 and 2.5, with hole diameters 12.7 and 11.7 mm, respectively. There were 13 or 19 holes in the array. Naphthalene was used and weighing of an hexagonal area surrounding the central hole was used to measure mass transfer. The relationship  $Sh_{L^*} = 1.196Re_D^{0.476}$  generalised the results [20]. Sherwood number was based on  $L^*$ , a dimension found from the area of the hexagonal naphthalene module divided by the hole pitch. This relationship was extrapolated to predict of Sherwood numbers for the pitch/diameter ratio of 88/56 investigated here. The dimension  $L^*$  for the boiler was 48.23 mm. For

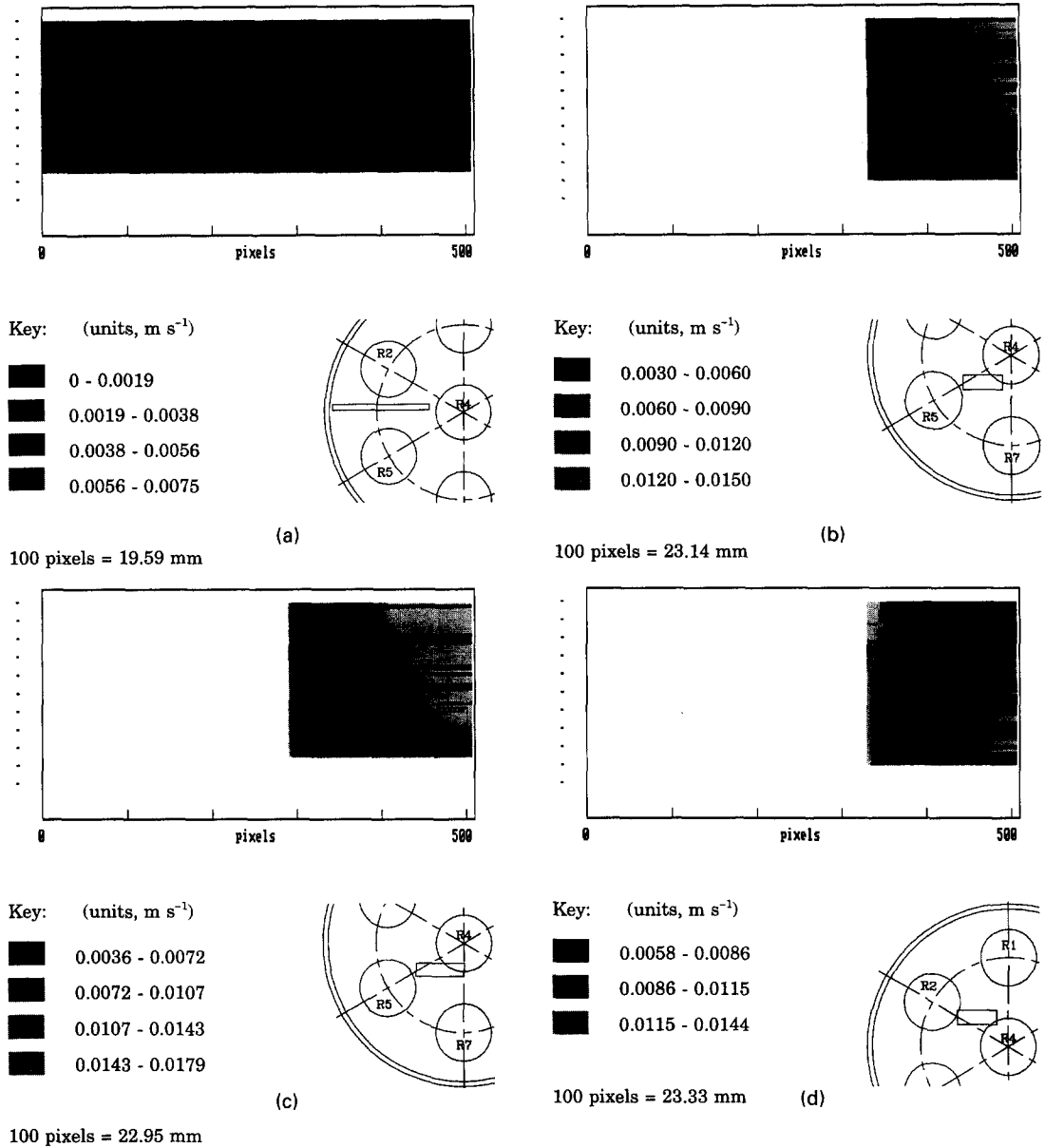


Fig. 6. Mass transfer contours over areas of ligament plate as located in Fig. 7 (original in colour).

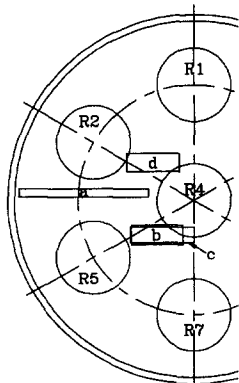


Fig. 7. Location of the areas examined on the ligament plate.

$Re_D$  of 5000 the predicted value for  $h_m$  was  $0.007 \text{ m s}^{-1}$ , for  $Re_D$  of 10 000 it was  $0.010 \text{ m s}^{-1}$  and for  $Re_D$  of 15 000 it was  $0.012 \text{ m s}^{-1}$ . These are average values but are comparable with the contour plots in Fig. 6.

The investigations using liquid crystals [21] examined an array of 39 mm diameter holes with pitch to diameter ratio 1.54. The seven holed plate studied was not flat but featured angled annular surfaces around the holes to model the weld in a practical system. Contours of heat transfer were obtained directly. For comparison of ref. [21] with mass transfer results here, the Chilton-Colburn analogy [1] can be used to convert the values:

$$Nu/Sh = (Pr/Sc)^{0.33}$$

Also



$$Nu/Sh = (hD/k)_{\text{boiler}} / (h_m D / D_m)_{\text{model}}$$

Thus

$$h/h_m = (Pr/Sc)^{0.33} (k_{\text{boiler}}/D_m)_{\text{model}} \quad (15)$$

For air at a typical boiler chamber temperature of 900 K,  $Pr = 0.70$  and thermal conductivity  $k$  is  $0.0615 \text{ W m}^{-1} \text{ K}^{-1}$ . At the temperature of the cold flow model 293 K, for a typical organic solvent in air  $Sc = 3.0$  and  $D_m$  is  $5 \times 10^{-6} \text{ m s}^{-2}$ . Using equation (15) gives  $h = 7632h_m$ .

It is reported [21] that for  $Re_D$  15 000 the value  $104 \text{ W m}^{-2} \text{ K}$  was observed above the central hole (which is equivalent to  $h_m$   $0.014 \text{ m s}^{-1}$ ) and  $83.6 \text{ W m}^{-2} \text{ K}$  was observed to the side and below the hole ( $\equiv h_m$   $0.011 \text{ m s}^{-1}$ ) decaying to around  $45 \text{ W m}^{-2} \text{ K}$  midway between the tubes ( $\equiv h_m$   $0.006 \text{ m s}^{-1}$ ). The values fell rapidly over the angled surface by 50%. These  $h_m$  values can be compared with Fig. 6(c) but the results here are for a flat surface and so total agreement would not be expected.

### CONCLUDING REMARKS

This technique has been developed to a stage where it can be used to provide data. Measurements were made for air jet impingement on a flat plate and for a model boiler. Both sets of results compared reasonably with the other published work, although in the flat plate studies observed mass transfer was lower than expected because these high mass flux experiments had extended beyond the end of the constant rate period. The technique is most useful with the present polymer and swelling agent for measuring mass transfer coefficients  $< 0.01 \text{ m s}^{-1}$ . In the model boiler, where the technique was more appropriately applied, mass transfer was observed to be significantly higher near the tube mouth than on other parts of the ligament plate. The contour maps which were obtained have shown that there is a distribution of mass transfer.

The technique is directly applicable in its present stage of development to problems where low accuracy is acceptable. The present optical system is attractively simple but further development would be needed if greater accuracy is required. The combined technique of swollen polymers with projected fringes is most likely to be useful in situations where relative measurements of mass transfer over a surface are required, rather than highly accurate absolute values at spot points. Where information is required directly in the form of mass transfer contours the technique would be particularly valuable. There are undoubtedly practical flat surface applications requiring elementary heat transfer measurements that could be provided by this robust and simple system. The method could be used to assess a situation without the need to use holographic equipment in the first instance. Proposed future work will look additionally at angled and curved surfaces. Laser glare observed on angled sur-

faces in some preliminary studies now under way suggests that there are difficulties to overcome in applying the technique to angled and curved surfaces.

System accuracy may be improved by use of a swollen polymer which permits greater surface recession during the constant rate period and so demands less of the optical system. Alternative polymer and swelling agent combinations have been tested. Polysulphide rubbers (e.g. Thiokol and Smooth-on) give high swelling with ethyl salicylate ( $\phi_{\text{sat}}$  about 0.5) so therefore much greater recession is permissible before the end of the constant rate period. However, there are problems in setting up the surface for study when using polymers which swell to this extent; designing a model of a complex surface to be coated with dry polymer is difficult. Polysulphide rubbers do not adhere well to metal backplates and they are generally beige or brown which makes them inferior as optical surfaces to white silicone polymer. A better solution which would extend the use of the swollen polymer technique is the identification of a swelling agent which has a higher diffusion coefficient  $D$  in the dry polymer so that the surface stays supplied even in high mass transfer situations for an adequate length of time. A swelling agent with a higher diffusion coefficient in silicone polymer than  $6.4 \times 10^{-11} \text{ m}^2 \text{ s}^{-1}$ , which is the value for isobutyl benzoate, is being sought. With the right agent, a high diffusion coefficient will be compatible with moderate ( $\phi_{\text{sat}} = 0.3$ ) swelling. Any new swelling agent is subject to the usual criterion of an appropriate vapour pressure, most usefully near  $4 \text{ N m}^{-2}$ . Research is continuing to identify a polymer and swelling agent combination with the required properties.

To summarise, the combined technique of swollen polymers with projected fringe measurement, as developed, is capable of providing useful data for a perforated flat plate in a model boiler. The technique could be applied to obtain mass and heat transfer coefficients at other flat surfaces such as are found in heat exchangers in industrial plant.

*Acknowledgements*—The National Advisory Body and Coventry University have funded this project. Thanks are due to British Gas M.R.S., Solihull for loan of equipment.

### REFERENCES

1. T. H. Chilton and A. P. Colburn, Mass transfer (absorption) coefficients. Prediction from data on heat transfer and fluid friction, *Ind. Engng Chem.* **26**(11), 1183–1187 (1934).
2. A. Larez and N. MacLeod, The axial and span wise variation of forced-convective transfer coefficient in the entrance region of a rectangular duct carrying a stream of air in transitional flow, *ICHEME Symp. Ser. No. 94*, 67–74 (1985).
3. J. H. Masliyah and T. T. Nguyen, Mass transfer due to an impinging slot jet, *Int. J. Heat Mass Transfer* **22**, 237–244 (1979).
4. N. Hay, Heat transfer measurement in steady state facilities. Part II: The swollen polymer technique, *Von Karman Institute for Fluid Dynamics Lecture Series* 1985-03

- Measurement Techniques in Turbo Machines*, Vol. 2, pp. 37–88 (25 February–1 March 1985).
5. M. R. Butcher, B. L. Button and C. C. Wright, A comparison of preliminary measurements of mass and heat transfer made in a tube, *Institution of Chemical Engineering 11th Annual Research Meeting*, pp. 153–158 (1984).
  6. W. R. Paterson, R. A. Colledge, J. I. MacNab and J. A. Joy, Solid–gas mass transfer measurement by the swollen polymer method: proving of swelling agents, *Int. J. Heat Mass Transfer* **30**(2), 279–287 (1987).
  7. N. MacLeod and R. B. Todd, The experimental determination of wall–fluid mass transfer coefficients using plasticized polymer surface coatings, *Int. J. Heat Mass Transfer* **16**, 485–504 (1973).
  8. N. MacLeod, The swollen polymer technique for mass transfer rate measurement at solid–fluid interfaces, submitted to *Int. J. Heat Mass Transfer*.
  9. M. R. Morshedizadeh and C. Wykes, Optical measurements of surface form using computer generated referencing, *J. Phys. E (Scient. Instrum.)* **22**, 88–92 (1989).
  10. D. N. Kapur and N. MacLeod, Vapour pressure determination for certain high-boiling liquids by holography, *Ind. Engng Chem. Product Res. Dev.* **15**(1), 50–54 (1976).
  11. L. R. G. Treloar, *The Physics of Rubber Elasticity* (3rd Edn), Chap. 7. Clarendon Press, Oxford (1975).
  12. D. N. Kapur, Profilometric determination of mass transfer coefficients by holographic interferometry, Ph.D. Thesis, University of Edinburgh (1973).
  13. R. A. Colledge, Heat and mass transfer at the wall of a packed bed at high Reynolds numbers, Ph.D. Thesis, University of Cambridge (1985).
  14. J. Crank, *The Mathematics of Diffusion* (2nd Edn). Clarendon Press, Oxford (1975).
  15. M. R. Morshedizadeh and C. Wykes, Computer aided surface topography measurement using phase stepping method. In *Advances in Manufacturing Technology IV—Proceedings of the 5th National Conference on Production Research* (ed. J. Chandler), pp. 77–81. Kogan Page (1989).
  16. C. A. Roberts, N. S. Girgis, J. R. Leech and I. V. F. Viney, Mass transfer from an opaque swollen polymer measured by a projected fringe optical technique, *Int. Commun. Heat Mass Transfer* **18**, 251–258 (1991).
  17. Y. Y. Cheng and J. C. Wyant, Phase shifter calibration in phase-shifting interferometry, *Appl. Optics* **24**(18), 3049–3052 (1985).
  18. C. O. Popiel and L. Boguslawski, Mass or heat transfer in impinging single, round jets emitted by a bell-shaped nozzle and sharp-ended orifice, *Proceedings of the 8th International Heat Transfer Conference (San Francisco)*, Vol. 3, pp. 1187–1192 (1986).
  19. C. A. Roberts, Mass transfer from swollen polymers measured by projected fringes, Ph.D. Thesis, Coventry University (1993).
  20. E. M. Sparrow and M. C. Ortiz, Heat transfer coefficients for the upstream face of a perforated plate positioned normal to an oncoming flow, *Int. J. Heat Mass Transfer* **25**, 127–135 (1982).
  21. S. Ashforth-Frost, R. J. Edwards, D. P. Graham, B. J. Lowesmith, K. Jambunathan and J. M. Rhine, Measurement of convective heat transfer coefficients, on the ligaments of a model shell boiler tube plate, using liquid crystal thermography, *ICHEME Symp. Ser. No. 129*, Vol. 1, p. 351 (1992).